JOURNAL OF THERMOPHYSICS AND HEAT TRANSFER
Vol. 14, No. 1, January–March 2000

Capillary Pumped-Loop Thermal Performance Improvement with Electrohydrodynamic Technique

B. Mo,* M. M. Ohadi,† and S. V. Dessiatoun‡
University of Maryland, College Park, Maryland 20742
and
K. R. Wrenn§
Swales Aerospace, Beltsville, Maryland 20705

The capillary pumped loop (CPL) is a state-of-the-art technology for cooling spacecraft and telecommunication devices. It is a two-phase heat-transport device in which the driving force is provided by the capillary action of the wick material in the evaporator. Compared to the widely used heat pipes, it provides a higher heat-transport capacity, more flexibility of installation, and greater heat-transport distance because of wickless transport lines and the absence of liquid and vapor counterflowing. The major disadvantages of the CPL are long and complicated startup procedures and the possibility of deprime at high heat input and large load variations. This paper investigates the liquid-vapor separation and thermal management with the electrohydrodynamic (EHD) technique for an EHD-assisted CPL using R-134a as the working fluid. An experimental investigation, along with a mechanism analysis, was employed to evaluate the potential of the EHD technique for thermal performance improvement of CPL systems. Experimental results showed that enhancements, up to three times, could be obtained in heat-transfer coefficients by applying an electric field at different heat load levels. The depriming conditions of a capillary pump can also be prevented with the EHD technique.

Nomenclature

A = surface area
a = object radius
E = electric field strength
F = electrohydrodynamic (EHD) force
h = heat-transfer coefficient
I = heater's current
i = discharge current
L = length
N = number of thermocouples
Q = heat-transfer rate or power
T = temperature
V = heater's voltage
ΔP = pressure drop
ϵ = permittivity
η = enhancement factor
κ = dielectric constant
ρ = density
ϕ = EHD potential

Subscripts

c = capillary
e = electric
g = gravity
h = heater
l = liquid or loop
ref = reference
t = total
v = vapor
w = wick or wall
0 = base case
1 = liquid phase
2 = vapor phase

Received 19 March 1999; revision received 13 September 1999; accepted for publication 16 September 1999.

*Research Assistant, Department of Mechanical Engineering; bmo@eng.umd.edu.
†Professor, Department of Mechanical Engineering.
‡Associate Research Scientist, Department of Mechanical Engineering.
§Thermal Engineer, Aerospace Products.

Introduction

THE capillary pumped loop (CPL) is a passively pumped two-phase heat-transport device that has demonstrated performance capabilities substantially greater than that of conventional, state-of-the-art heat pipes. It transports a large heat load over long distances with very small temperature differences in the system. The driving force for the CPL loop is surface tension forces developed in porous wicks located within the evaporator.[1] Like other heat-transfer devices, the CPL is limited by a maximum amount of heat that can be transported from the evaporator end to the condenser end of the system. The capillary limit is again a major concern similar to conventional heat pipes, expressed as

$$(\Delta P_c)_{\max} = \Delta P_v + \Delta P_l + \Delta P_w + \Delta P_g \tag{1}$$

Acquisition of heat at the evaporator provides the driving force in a CPL system. Therefore, the capillary pump is the primary element for heat acquisition. For a given heat input to the CPL, the total pressure drop in the loop must not exceed the capillary pumping head if the CPL is to work properly. The wick meniscus will also adjust itself so that the capillary pressure equals the loop pressure drop.

The other limit, more specific to the operation of the CPL, is the liquid line boiling limitation.[2] Between the evaporating and absorbing surface of the wick, a pressure spike is actually observed because of superheated liquid boiling. A pressure rise is required to match the pressure surge, observed as the liquid is pushed from the vapor line.[3] The pressure drop through the wick can be minimized to prevent boiling. The Clausius–Clapeyron equation is appropriate for determining subcooling requirements. The liquid line boiling limitation is reinforced through the liquid subcooling after condensation to avoid boiling in the liquid line. It is also related to the liquid pressure drop. Kolos and Herold[4] performed detailed analysis for the observed oscillatory fluid motion in the capillary evaporator core.

Above the capillary pump limit, ensuring that the loop is still working properly or developing a vapor-tolerant CPL system becomes a challenge. Babin et al.[5] investigated an ion-drag

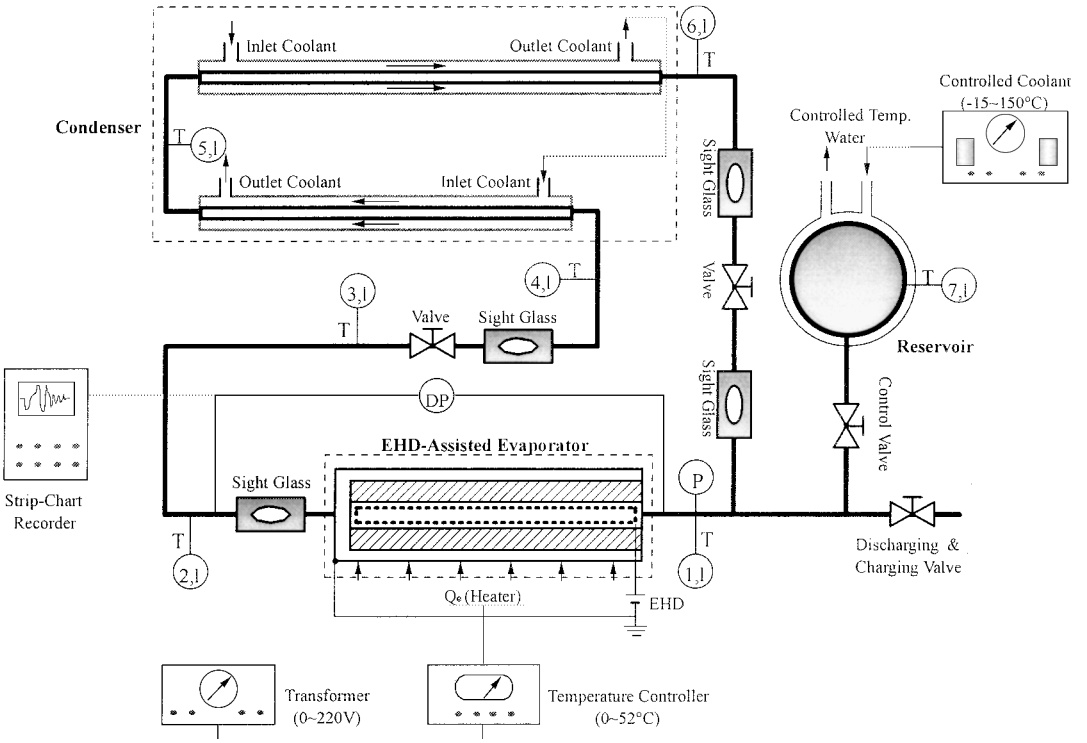

Fig. 1 Schematic of the EHD-assisted CPL.

pump-assisted capillary loop. Up to 100% improvement of the heat transport capacity and about 70 Pa of maximum electrohydrodynamic (EHD) pressure head were reported. Bryan and Seyed-Yagoobi[6] studied the monogroove heat pipe with EHD pumping. Combination of the capillary and EHD forces yielded 320 Pa of pressure head at an applied potential of 20 kV. Ohadi et al.[7,8] investigated the feasibility of the EHD-assisted CPL. Significant improvements in the liquid pumping capacity and the evaporative heat-transfer coefficient, using EHD in a CPL equivalent system, were experimentally demonstrated. Mo et al.[9,10] figured out the potential of heat-transfer enhancement and the startup time reduction for an EHD-assisted CPL. Using EHD effects of liquid-vapor separation, this paper identifies the potential of the heat-transfer enhancement and the prevention of deprime condition on an EHD-enhanced CPL system.

EHD is a new and promising technique that has demonstrated potential for significantly reducing the heat-exchanger size/volume while providing on-line/on-demand control for the heat-transfer surface. Its applicability for substantial increase of heat-transfer coefficients of industrially significant fluids such as refrigerants R-134a, R-123, Poly Alphaolefin, and certain aviation fuels has already been proven. Polarized EHD force (pumping) can also assist or substitute capillary forces to collect, guide, and pump condensate in regions of high electric field intensity, whereas the saturated vapor of the dielectric fluid is repelled to locations where the electric field is less intense. Because of the dominance of polarization EHD force over surface tension forces, the dielectrophoresis phenomenon may significantly improve the heat-transfer capability of two-phase flow thermal devices using dielectric fluids with poor surface tension. The potential terrestrial applications of the EHD technique are extensive and include commercial heat-exchanger equipment for refrigeration and air conditioning, electronic cooling, cryogenic and process industry applications, and laser medical/industrial cooling.

An on-line/on-demand control feature to the heat-transfer surface is provided because the magnitude of heat-transfer enhancement in the EHD technique is directly proportional to the applied voltage. This feature is particularly attractive for developing higher heat-transfer capacity and vapor-tolerant CPL systems. In addition to improving the heat transfer, EHD coupling will also enhance CPL startup procedure. These merits further promote the readiness of CPL technology for space thermal control applications.

Experimental Apparatus

The schematic diagram of the EHD-assisted CPL setup used in the current experiments is shown in Fig. 1. The key component of the setup is the EHD-assisted evaporator. The heater for the evaporator was designed for a maximum allowable heat-transport capacity of 1500 W. The working fluid in the experiments reported here was the environmentally acceptable R-134a (HFC-134a). Other major components included the cooling loop, the control (reservoir) loop, and the various auxiliary instrumentations for monitoring and control of the depriming conditions. A brief description of the main components of the experimental apparatus is given in the following sections.

EHD-Assisted Evaporator Test Section

An EHD-assisted evaporator was designed and fabricated to simulate conditions in a spacecraft CPL system. A 25.4-mm CPL pump (evaporator) was modified to realize the EHD-assisted test section. It was oriented horizontally in the loop. The wick structure material in the evaporator was polyethylene. As shown in Fig. 2, a spring-type (helical) electrode was inserted into the liquid channel of the evaporator to implement EHD-assisted performance. The axial pitch of the spring electrode was about 1 mm. The outer diameter of the spring was 12 mm, nearly the same as the inside diameter of the wick structure. The grooved aluminum tubing served as the ground electrode, whose inside diameter was 15.4 mm. The gap of the electrodes then was 6.35 mm. A heater was placed at the surface of the evaporator. The outer surface area of the wick was 202 cm^2. A total of 14 thermocouples (T_{1-14w}), as shown in Fig. 3, were mounted along the outside wall of the evaporator to measure the average wall temperature. Differential pressure measurement was used to evaluate the evaporator behavior in the loop. Seven additional thermocouples (T_{1-71}) were placed in the loop to measure temperatures at various points on the loop, as shown in Fig. 1. The electrode for applied high-voltage electric field was inserted in the liquid side of the wick. The voltage potential was applied via a laboratory-grade high-voltage supply. The applied electric field enhanced the transfer of liquid across the wick to the evaporator surface.

Capillary force in the wick of evaporator provides the pumping head required for the CPL. Menisci, which adjust naturally to

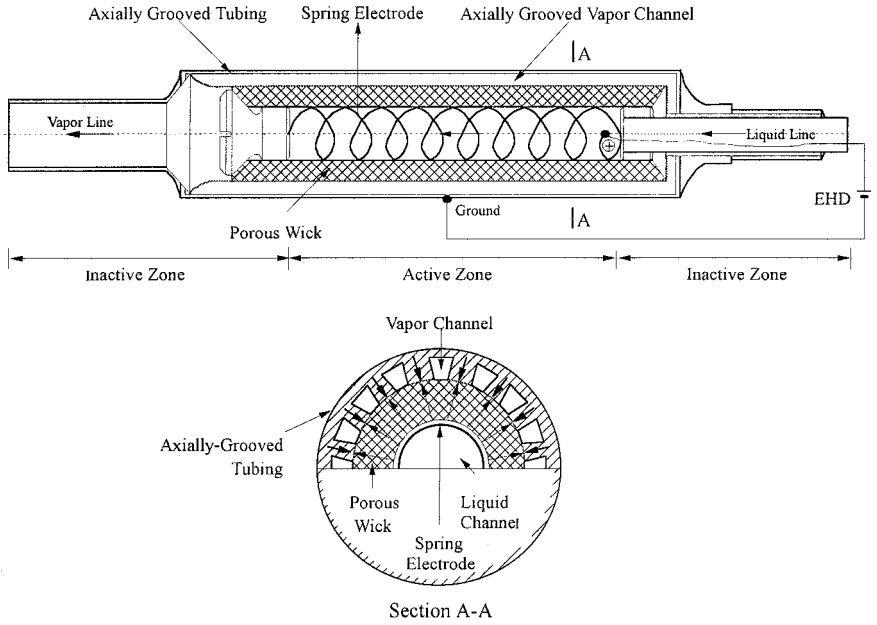

Fig. 2 Schematic of the EHD-assisted capillary evaporator.

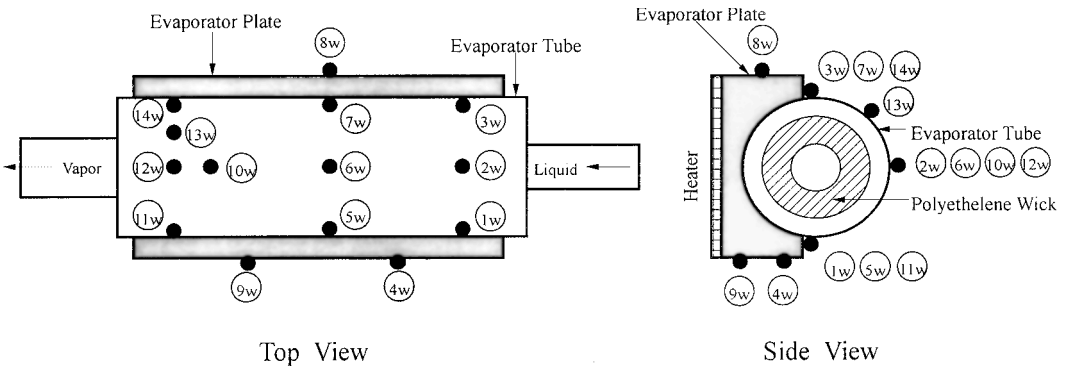

Fig. 3 Surface temperature measurement at capillary evaporator.

provide the proper pumping head required to match the flow losses associated with the applied heat input and condenser conditions, are formed at the liquid–vapor interface in the evaporator. The wick used in the current experiments was a sintered porous ultra-high-molecular-weight polyethylene, with nominal diameter of 15μ. The wick permeability ranged from 10^{-14} to 10^{-12} m^2, with a porosity of 50% and a low thermal conductivity.

Cooling (Condensing) Loop

The stability of the EHD-assisted CPL setup was maintained using a cooling (condensing) loop. Cold water generated by the chiller circulated in the condenser side and removed the heat generated as a result of the phase change process in the evaporator.

Control (Reservoir) Loop

The function of the reservoir in the CPL system was to control the operating temperature and facilitate the startup procedure for the loop. Instead of an electric heater, a small chiller with temperature control was installed on the reservoir.

Different Depriming Condition Control

Two adjustable valves were arranged at the liquid line and vapor line of the CPL loop. At different power levels, by adjusting the opening of the two valves, the depriming conditions were triggered. As shown in Fig. 1, four custom-designed sight glasses were installed in the system to better visualize the loop operation.

Experimental Procedure

A typical experimental procedure began by turning on the two-chiller system. When the reservoir temperature reached the operating temperature, the power to the evaporator was applied to start up the CPL system. After the loop operation stabilized, the high-voltage electric field was applied to realize the EHD effect.

Next, the system was allowed to reach steady-state conditions where the fluctuations in wall temperatures and the average differential pressure reading were less than 1% of average readings. Then the local wall temperatures along the test section, the loop temperatures, and the high-voltage current were measured. Depending on the type of parametric study, the condition settings were changed accordingly for the next data point. The procedure was repeated until completion of the experimental run.

Data Reduction

The average wall temperature of the evaporator is calculated using the following equation:

$$T_w = \sum_{i=1}^{N} T_{w,i} \Big/ N \tag{2}$$

The heat-transfer rate Q_h of the test section is evaluated by

$$Q_h = V \times I \tag{3}$$

The test section was well insulated, and heat losses to the surroundings were estimated to be negligible. Then the heat-transfer

coefficient can be defined as

$$h = \frac{Q_h}{A \times (T_w - T_{\text{ref}})} \tag{4}$$

(T_{eff} taken as the reservoir temperature corresponding to the system operating temperature).

The enhancement factor η is then defined as

$$\eta = h / h_0 \tag{5}$$

The ratio of EHD power consumption to the total heat transferred to the test section is calculated as

$$\frac{Q_{\text{EHD}}}{Q_{\text{Total}}} = \frac{Q_{\text{EHD}}}{Q_h + Q_{\text{EHD}}} \tag{6}$$

Analysis of the various operating temperatures and system deprime conditions is achieved by collecting data by the various differential pressure transducers, evaporator wall and loop temperatures, applied voltage and current, and other auxiliary measurements at various points in the loop.

The evaluation of uncertainty is based on the fact that a differential change of a function can be expressed in terms of the differential change of the dependent variables and the partial derivatives with respect to the corresponding dependent variables. Measurement errors for the current experiments were the following: temperature ±0.1°C, pressure ±0.1% of the reading, heater voltage ±0.5% of the reading, heater current ±0.1% of the reading, applied EHD voltage ±0.1% of the reading, and applied EHD current ±0.1% of the reading. The analysis showed that the uncertainty in the heat-transfer rate Q_h was ±1.35%, and the uncertainty in the heat-transfer coefficient h was from ±2.86% to ±11.8% with the higher uncertainty corresponding to the lower heat flux. The uncertainty in power consumption Q_{EHD} was ±1.74% to ±5.16%, where again the larger uncertainty is associated with the lower heat-flux levels.

Results and Discussion

Heat-Transfer Coefficient Enhancement

On the normal condition the potential of the heat-transfer coefficient enhancement with the EHD assistance was first identified. When applying an electric field, the wall temperatures at the evaporator would decrease. Therefore the heat-transfer coefficient would increase accordingly. Figure 4 shows the EHD-enhanced heat-transfer coefficient and enhancement ratio as a function of applied voltages. As illustrated there, up to two-and-one-half-times enhancement can be obtained at 9 kV applied high voltage. Similar enhancement trends for power levels 600, 625, and 650 W are seen in Fig. 5, where up to three times heat-transfer coefficient enhancement is obtained. The results confirm a previous feasibility study finding that EHD is applicable in an actual CPL system.[7]

The heat-transfer coefficient reaches the maximum value at around 525 W power level. The heat-transfer coefficient above and

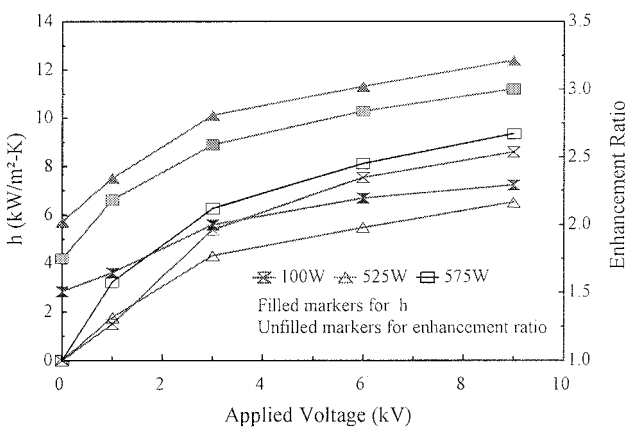

Fig. 4 Heat-transfer coefficient and enhancement ratio: 100, 525, and 575 W.

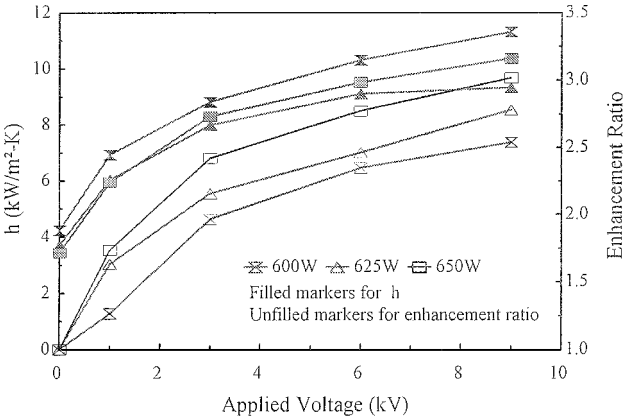

Fig. 5 Heat-transfer coefficient and enhancement ratio: 600, 625, and 650 W.

below 525 W is lower for the base case (without EHD). This is because the pressure head generated in the evaporator pump at the 525 W level is at its optimum condition. The liquid-vapor interface inside the evaporator wick is at the optimum position from the viewpoint of CPL pressure head limit and boiling limit. However, above 525 W, the EHD-induced heat-transfer enhancement is higher. The highest three times enhancement is obtained for 650 W. Also, The EHD power consumption is on the order of 50 mW, which translates into a maximum value of 0.1% EHD power consumption ratio. Compared with the power input levels (100–650 W), the EHD power consumption is clearly negligible.

Three major factors attribute to the liquid-vapor separation and performance enhancement by using the EHD technique. They are EHD-affected bubble behavior, electrothermally induced EHD pumping and EHD-induced Maxwell stresses.[11] These EHD effects can be used in heat pipes or CPL for the performance improvement.

For the vapor bubble in a nonuniform electric field, Pohl[12] showed that the excess EHD force on a small spherical object of dielectric constant κ_1 in a dielectric fluid of dielectric constant κ_2 was given as

$$F_e = 2\pi a^3 \kappa_1 \varepsilon_0 \frac{\kappa_2 - \kappa_1}{\kappa_2 + 2\kappa_1} \nabla E^2 \tag{7}$$

This relation indicates that the motion of the sphere under the influence of the nonuniform electric field will be proportional to the difference of the dielectric constants and the divergence of the electric field strength. It was derived from the ideal case, where only one bubble was present in the liquid pool. For the specific cases the trends, where the fluid with a higher dielectric constant will always move toward the stronger field strength and vice versa, will be the same.

The electrothermally induced EHD pumping effect, when combined with bubble-modification caused by the Maxwell stresses, results in liquid-vapor separation phenomenon, which leads to improved pumping head at the evaporator wick and performance improvement of an EHD-assisted CPL system.

The deprime of a capillary pump (evaporator) is referred to the condition that an evaporator is no longer able to pump working fluids in the loop. The evaporator will be starved of liquid because of insufficient flow of vapor on the liquid side of the wick. The vapor may be pushed into the liquid core of the evaporator under the deprime condition. Thus a deprimed evaporator will not transport heat because the evaporator cannot generate pumping heat to circulate the working fluid. Accumulation of vapor bubbles in the evaporator core attributes to the CPL deprime under certain high heat load operations.

When applying an electric field, the induced Maxwell stresses at the liquid-vapor interface, combined with the electrothermally induced pumping effect, make the liquid surface rise, resulting in lifting of the liquid-vapor interface in the direction of the ground electrode (evaporator plate), as seen in Fig. 6. Furthermore, EHD also repels the vapor bubble to a less intense electrical field, which is

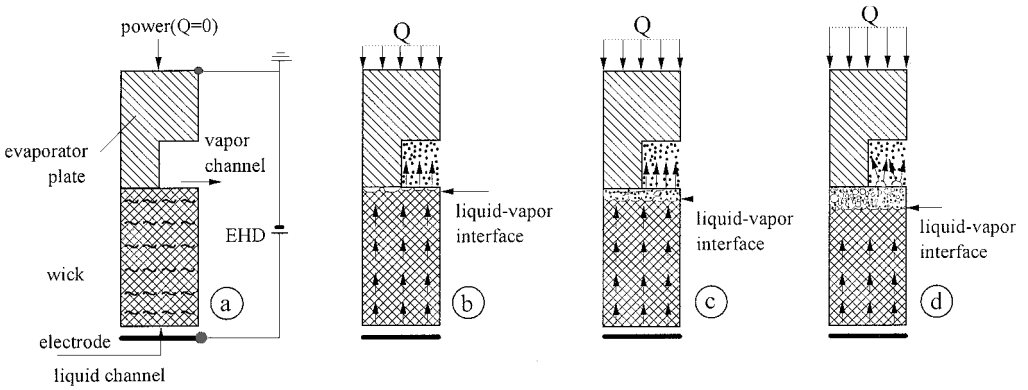

Fig. 6 CPL evaporator behavior at different power level (in presence of the EHD condition).

away from the charged electrode and toward the evaporator surface. All of those EHD effects collaborate to enhance heat transfer.

As shown in Fig. 6b, at normal operation of given power level Q, the liquid-vapor interface moves up to vapor channel and affects the effective wick radius, thus enhancing the heat-transfer coefficient. These EHD effects of liquid-vapor separation are the major mechanism for the heat-transfer enhancement at the normal operating conditions. To prevent depriming conditions, as shown in Figs. 6c and 6d, liquid-vapor interface moves up to the wick structure, and more bubbles are repelled away and out into vapor channel. The effective wick radius will be delayed in reaching its limit of the minimum value (pore radius). Thus the higher EHD-induced heat-transfer enhancement will be expected for the high heat load levels, as observed at 650 W power level.

Deprime Condition Prevention

When the effective wick radius reaches its limit of minimum value, a depriming condition will occur for a CPL with further heat input. In our experimental setup the opening of two valves at the liquid line and vapor line was adjusted to trigger deprime conditions at different valve positions. For the predefined depriming condition a corresponding heat load was applied first. Then the openings of the two valves were slowly adjusted until the deprime occurred. After that the heat input was turned off. The loop was restarted with the already determined opening positions of the two valves. The predefined heat load was applied again to verify the occurrence of the deprime phenomenon. Finally, the openings of the two valves for the depriming condition were identified. Instead of adjusting operating temperature or power level to trigger the deprime, this method could provide the same power level depriming condition for different tested working fluids. In the following the data of R-134a for the deprime prevention at 150 and 300 W depriming conditions are discussed.

Figures 7a and 7b show the experimental result on the 150-W depriming condition. From the readings of the differential pressure (DP), evaporator wall and loop temperatures, realization of the vapor-tolerant properties with 15 kV applied voltage is demonstrated. Seen there without the applied high voltage, the evaporator wall and loop temperatures kept rising with the elapsed time, which eventually would lead to the occurrence of deprime. Then 15-kV high voltage was applied, these temperatures dropped, and finally the loop operated in the stable status. The deprime was prevented. With the reduction of the power level to 100 W, the loop still operated normally.

Figures 8a and 8b show the similar results for a 300-W depriming condition. The vapor-tolerant system is achieved with 18-kV applied voltage. Furthermore, the observation was made that the loop would deprime again at the reduced 250-W power level (at around 320 min) without applying an electric field after EHD had already prevented the depriming condition at 300 W. This means that EHD can only tolerate the vapor bubbles during the depriming condition, but cannot collapse or break the big vapor bubbles. The loop only operated normally again until the further reduction of power to 200 W.

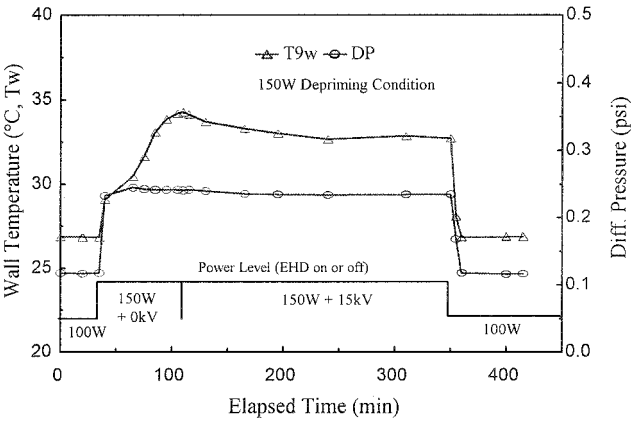

Fig. 7a Variation of DP and evaporator wall temperature (#9): 150-W depriming condition.

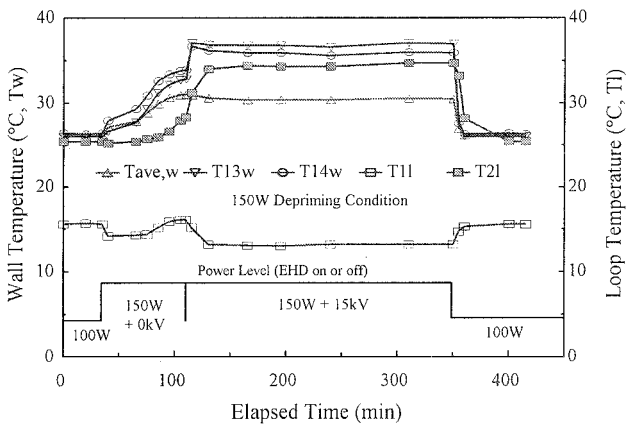

Fig. 7b Variation of evaporator wall and loop temperatures: 150-W depriming condition.

On the partial depriming condition before applying EHD, as shown in Fig. 9a, vapor may penetrate some parts of the wick while the liquid occupies other parts of the wick. Some small vapor bubbles will also appear in the liquid line of the evaporator.

When an EHD is applied, the trends of repelling vapor to a less intense electric field may collect small bubbles together. However, EHD effects are not strong enough to collapse or break them. After some time at the vapor partially penetrating location, bubbles will be at equilibrium under forces of EHD extraction, capillarity, and gravity. No small bubbles will exist in the liquid line. The bigger bubbles present at the original vapor partially penetrating location will keep relatively stable, as seen in Fig. 9b. If the EHD effect is turned off, the loop will deprime again even though the power level is reduced because of the vapor appearing between the wick and the

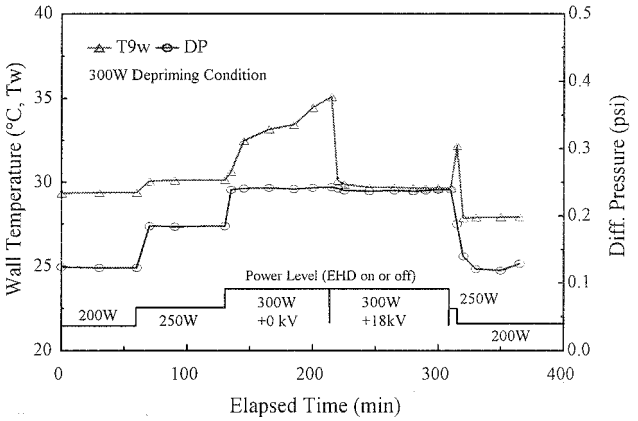

Fig. 8a Variation of DP and evaporator wall temperature (#9): 300-W depriming condition.

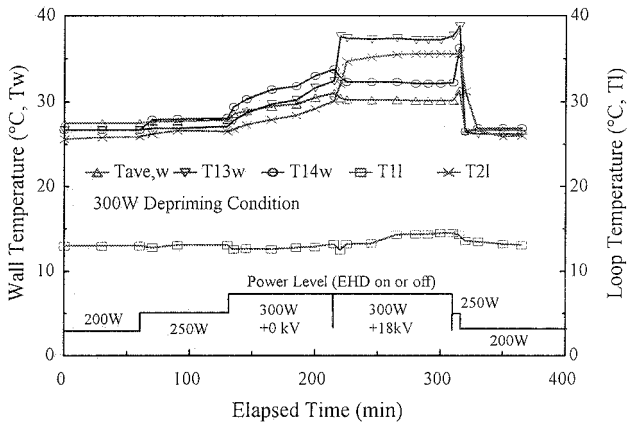

Fig. 8b Variation of evaporator wall and loop temperatures: 300-W depriming condition.

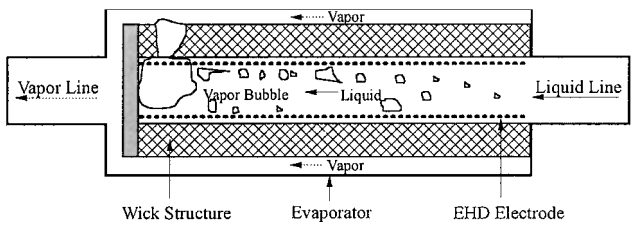

a) No EHD condition

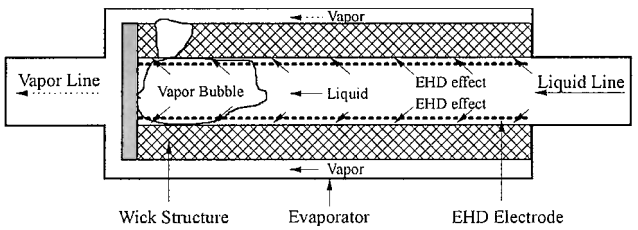

b) EHD condition

Fig. 9 Different bubble behaviors under EHD on and off.

liquid line. In summary, the EHD vapor tolerance is achieved by preventing further growth and penetration of bubbles in the liquid line and the wick.

Conclusions

Like other heat-transfer devices, the CPL is limited by a maximum amount of heat that can be transported from one end to the other. The capillary limit is a major concern, as is the case in conventional heat pipes.

An experimental investigation along with analysis of the controlling mechanism was employed to evaluate the potential of the EHD technique on CPL thermal performance improvement. Experimental results showed that up to three times heat-transfer enhancement could be obtained by applying an electric field at different heat load levels. When EHD is applied to a phase-change process, liquid phase and vapor phase will behave differently because of their different dielectric properties. Thus, the liquid-vapor separation can be realized by using the EHD technique. Furthermore, Maxwell stresses combined with an electrothermally induced pumping effect assist the capillary force to improve the wick performance inside the evaporator. Experimental data also revealed that the deprime condition of a capillary pump can be prevented in the presence of an electric field. In general, the results of the present experiments suggest that with proper electrode design an EHD-assisted CPL can be vapor tolerant and benefit from improved reliability while exhibiting substantially improved thermal performance.

Acknowledgments

Financial support of this work by a consortium of sponsoring members is greatly acknowledged. Technical assistance and laboratory support by the Swales Aerospace, Beltsville, Maryland, and the efforts of Eric Haught and Marc Kaylor in this regard were particularly essential to successful completion of this work. Thanks also go to Majid Molki of our group for his critical review of this paper.

References

[1]Ku, J., "Recent Advances in Capillary Pumped Loop Technology," AIAA Paper 97-3870, Aug. 1997.

[2]Maidanik, Y., Solodovnik, N., and Fershtater, Y., "Experimental and Theoretical Investigation of Startup Regimes of Two-Phase Capillary Pumped Loops," Society of Automotive Engineers, Paper 93-2305, July 1993.

[3]Hoang, T., and Ku, K., "Theory of Hydrodynamic Stability for Capillary Pumped Loop," *Proceedings of 31st National Heat Transfer Conference*, HTD-Vol. 307, American Society of Mechanical Engineers, 1995, pp. 33–40.

[4]Kolos, K. R., and Herold, K. E., "Low Frequency Temperature and Fluid Oscillations in Capillary Pumped Loops," AIAA Paper 97-3872, Aug. 1997.

[5]Babin, B. R., Peterson, G. P., and Seyed-Yagoobi, J., "Experimental Investigation of an Ion-Drag Pump Assisted Capillary Loop," *Journal of Thermophysics and Heat Transfer*, Vol. 7, No. 2, 1993, pp. 340–345.

[6]Bryan, J. E., and Seyed-Yagoobi, J., "Heat Transport Enhancement of Monogroove Heat Pipe with EHD Pumping," *Journal of Thermophysics and Heat Transfer*, Vol. 11, No. 3, 1997, pp. 454–460.

[7]Ohadi, M. M., Dessiatoun, S. V., Mo, B., Kim, J., Cheung, K., and Didion, J., "An Experimental Feasibility Study on EHD-Assisted Capillary Pumped Loop," *Space Technology and Applications International Forum, American Institute of Physics Conference Proceedings*, Vol. 387, Pt. 2, AIP Press, Woodbury, NY, 1997, pp. 567–572.

[8]Ohadi, M. M., Dessiatoun, S. V., and Mo, B., "An EHD-Assisted Capillary Pumped Loop," EHD Aerospace Consortium, Enhanced Heat Transfer Lab., Univ. of Maryland, Progress Rept. 6, College Park, MD, Feb. 1997.

[9]Mo, B., Ohadi, M. M., and Dessiatoun, S. V., "Liquid-Vapor Separation and Thermal Management in an EHD-Enhanced Capillary Pumped Loop," *Heat Transfer 1998, Proceedings of 11th International Heat Transfer Conference*, Vol. 2, Taylor and Francis, Inc., Levittown, PA, 1998, pp. 63–68.

[10]Mo, B., Ohadi, M. M., Dessiatoun, S. V., and Cheung, K., "Start-Up Time Reduction in an Electrohydrodynamically Enhanced Capillary Pumped Loop," *Journal of Thermophysics and Heat Transfer*, Vol. 13, No. 1, 1999, pp. 134–139.

[11]Melcher, J. R., *Continuum Electromechanics*, MIT Press, Cambridge, MA, 1981, pp. 5.45–5.54.

[12]Pohl, H. A., *Dielectrophoresis—The Behavior of Neutral Matter in Non-Uniform Electric Fields*, Cambridge Univ. Press, New York, 1965, pp. 63–69.